Machine Learning Identifies Microbiome and Clinical Predictors of Sustained Weight Loss Following Prolonged Fasting

Gelsomina N. Kaufhold[1,2,3,*], Theda U. P. Bartolomaeus[1,2,3,4,*], Kristin Kräker[1,2,3,4], Till Schütte[1,2,3,4], Sakshi Kamboj[5], Ulrike Löber[1,2,3,4], Gabriele Rahn[1], Victoria McParland[1,3,6], Lena Braun[1], Lajos Markó[1,2,3,4], Matanat Mammadli[1,2,3], Alexander Krannich[7], Lina S. Bahr[1,2,3], Friederike Gutmann[1,2,3,4], Friedemann Paul[1,2,3], Nicola Wilck[1,3,4,6], Alma Zernecke[8], Peter J. Oefner[5], Wolfram Gronwald[5], Dominik N. Müller[1,2,3,4], Sofia K. Forslund-Startceva[1,2,3,4,9], Sylvia Bähring[1,2,3,†], Hendrik Bartolomaeus[3,4,8,†], Nadja Siebert[1,2,3,†]

[1]Experimental and Clinical Research Center (ECRC), a cooperation of Charité - Universitätsmedizin Berlin and Max Delbrück Center for Molecular Medicine, Berlin, Germany

[2]Charité-Universitätsmedizin Berlin, corporate member of Freie Universität Berlin and Humboldt-Universität zu Berlin, Berlin, Germany.

[3]Max Delbrück Center for Molecular Medicine in the Helmholtz Association (MDC), Berlin, Germany

[4]DZHK (German Centre for Cardiovascular Research), partner site Berlin, Germany

[5]Institute of Functional Genomics, University of Regensburg, Regensburg, Germany

[6]Department of Nephrology and Internal Intensive Care Medicine, Charité –Universitätsmedizin Berlin, Germany.

[7]BioStats GmbH, Nauen, Germany

[8]Institute of Experimental Biomedicine, University Hospital Würzburg, Germany.

[9]Structural and Computational Biology Unit, European Molecular Biology Laboratory (EMBL), Heidelberg, Germany.

*contributed equally

†jointly supervised the work

Correspondence: bartolomae_h@ukw.de

Abstract

Prolonged fasting may benefit metabolic health, but data in healthy individuals remain limited. We performed a randomized, waitlist-controlled study (LEANER study), with 38 healthy participants completing a 5-day-fasting intervention with 12-week follow-up. Fasting acutely lowered body mass index (BMI), via fat mass loss. These changes partially persisted at follow-up. Fasting altered the gut microbiome composition and induced metabolite shifts in plasma and feces. Changes to gut microbiome alpha diversity after fasting correlated with baseline microbiome diversity. Long-term BMI response at follow-up could be predicted through machine learning (ML) using baseline microbiome and clinical data, highlighting an unknown *Faecalibacterium* sp., *Oscillibacter* sp. 50_27, LDL cholesterol, and systolic blood pressure as key predictors. This ML model was validated in independent patient cohorts with metabolic syndrome and multiple sclerosis. These findings support prolonged fasting as an effective metabolic intervention and demonstrate that individual responses to fasting interventions can be predicted using pre-intervention features.

Trial registration: ClinicalTrials.gov, NCT04452916. Registered on June 26, 2020

Key words: fasting, gut microbiome, weight loss, machine learning, personalized nutrition, precision medicine

Introduction

Fasting interventions have gained renewed attention for their potential to modulate metabolism, reshape the gut microbiome, and promote healthy aging[1]. While fasting protocols vary widely from time-restricted eating to fasting-mimicking diets[2], and prolonged food abstinence lasting up to several weeks (up to 26 days)[3], the underlying principle is consistent: transient caloric deprivation triggers coordinated physiological responses that may confer long-term health benefits[4].

Evidence from patient populations, including those with metabolic syndrome[5], autoimmune diseases[6,7], and cancer[8], suggests that fasting can influence key regulatory pathways such as autophagy, insulin sensitivity, and oxidative stress[1]. In individuals with metabolic syndrome, we previously demonstrated that a 5-day fast atop a DASH (Dietary Approaches to Stop Hypertension) diet induced profound and coordinated changes in gut microbiome composition and immune cell states most of which were reversed at 12 weeks follow-up[5]. Using immune cell population or microbiome profiles, we developed models that predicted long-term antihypertensive effects, supporting the concept of data-driven stratification[5].

In parallel, gut microbiome profiling has emerged as a powerful tool for personalized medicine[9]. Microbial signatures have been linked to energy metabolism[10], weight regulation[11,12], and immune modulation[13,14]. Personalized dietary approaches that account for microbiome composition have demonstrated superior outcomes in metabolic control[8]. Emerging applications extend to autoimmune, neuropsychiatric, and oncologic indications, underscoring the potential of microbiome-informed strategies in precision medicine[9,15].

Despite these advances, the long-term effects of prolonged fasting in healthy individuals remain poorly characterized. Most existing studies rely on non-randomized designs, lack adequate control groups, or fail to include follow-up assessments. Furthermore, many

interventions are performed in multimodal clinical settings involving exercise, psychological support, and dietary coaching[5], making it difficult to isolate the effect of fasting alone.

Here, we present a randomized, waitlist-controlled study investigating the effects of a 5-day prolonged fasting intervention in healthy adults, with follow-up assessments at 12 weeks. We integrated clinical, microbiome, and metabolome profiling to characterize immediate and long-term physiological responses. Using machine learning, we show that sustained weight loss can be predicted from baseline microbiome and clinical features. The results that were validated in independent cohorts with metabolic syndrome and multiple sclerosis. Our findings offer mechanistic insight into fasting responses and support the potential of microbiome-informed strategies for personalized lifestyle interventions.

Results

Prolonged fasting affects energy expenditure and long-term weight loss

Thirty-eight healthy participants were recruited for a 5-day prolonged fasting intervention (Figure 1a). As fasting interventions cannot be blinded, we decided to use a waiting list control to account for physiological fluctuations within a 12-week timeframe while maximizing the number of participants undergoing prolonged fasting (Figure 1A). Baseline characteristics are shown in Table 1.

Of the 38 participants, 83% reported fasting-related adverse events (AE) (Table S1). All AE were mild and transient and did not necessitate discontinuation of fasting. Blood glucose and β-hydroxybutyrate levels were measured each morning and evening during the five-day fasting period (days 1–5), confirming that all participants adhered closely to the study protocol (Figure S1a, b). We observed a diurnal rhythm with higher BHB but lower glucose concentrations in the morning compared to the evening (Figure S1a, b). Continuous interstitial glucose monitoring during the five-day fasting period, compared with baseline measurements and waiting-list controls, confirmed a dynamic reduction in glucose levels over the course of the fast. (Figure 1b). Following refeeding the glucose levels normalized; however, between days 2 and 4 post-fast, blood glucose concentrations were elevated throughout the day (06:00–22:00) compared with baseline measurements (Figure 1c).

Our predefined endpoint was a change in resting energy expenditure (REE). Prolonged fasting acutely reduced REE by 62 kcal/d, suggesting a fasting-induced, energy-preserving mechanism (Figure 1d, Supplementary Data 1). We did not observe alterations in REE between the two baseline timepoints of waiting list controls (Figure 1d). Since REE was the defined endpoint, we performed a linear mixed model showing that lean mass ($p < 0.001$) and not self-reported sex significantly influenced REE at all visits, including post-fasting

106 (Figure S2). Following the five-day fast, respiratory exchange ratios (RER) declined
107 significantly (Figure 1e), paralleling a peak in BHB concentrations on day 5 (Figure S1b). All
108 those metabolic makers returned to baseline by 12 weeks post-fast.
109 Furthermore, we observed that prolonged fasting reduced BMI (Figure 1f). This decrease was
110 partly reversed after 12 weeks follow-up (Figure 1f). Body composition analysis attributed
111 this incomplete return towards baseline BMI predominantly to a reduction in fat mass
112 (Figure 1g, S1g). Of note, the absolute and relative reduction of body fat was accompanied
113 by a reduction in lean mass during fasting that completely reverted at follow-up (Figure S1h).
114 Prolonged fasting reduced waist-to-hip ratio and diastolic blood pressure while increasing
115 heart rate, findings which are consistent with a previously published study in metabolic
116 syndrome (Figure S1d-g). In contrast to metabolic syndrome patients[5], the healthy
117 participants in this study did not exhibit sustained blood-pressure reductions (Figure S1e, f).
118 Taken together, these results demonstrate that prolonged fasting is well tolerated in healthy
119 individuals, yielding sustained reductions in BMI and fat mass, while most metabolic and
120 hemodynamic parameters return to baseline during the 12-week follow-up.
121
122 *Prolonged fasting induces large short-term and small long-term changes in gut microbiome*
123 *composition*
124 To assess the natural fluctuation of the gut microbiome composition, we analyzed changes
125 between the two baseline samples (baseline 0 and baseline 1) from the waiting list control
126 (Figure 1a). Microbial alpha diversity, measured as Shannon index, and microbiome
127 composition quantified by Bray-Curtis dissimilarity did not differ significantly between the
128 two baseline samples (Figure S3a, b). Shannon index remained stable across all study visits
129 (Figure 2a). In contrast, individual trajectories in response to fasting varied markedly (Figure

130 2a). Interestingly, short-term (post-fasting) and long-term (follow-up) changes in alpha-
131 diversity correlated negatively with alpha-diversity at baseline, implicating baseline
132 differences in microbiome composition as relevant predictors of fasting-induced microbiome
133 changes (Figure 2b, c). Bray-Curtis dissimilarity-based multivariate analysis of the taxonomic
134 composition demonstrated a significant shift in microbial community composition in
135 response to fasting that partially reversed during the follow-up period (Figure 2d). Consistent
136 with the observed shift in the multivariate analysis, fasting induced significant changes in
137 several bacterial species that reversed during follow-up. For example, *Roseburia* sp. inserta
138 sedis and *Bifidobacterium adolescentis* decreased after the fasting period but increased at
139 follow-up, whereas *Faecalibacterium* sp. CAG-74 showed the opposite pattern (Figure 2e,
140 S3c, Supplementary Data 2). In contrast, only seven taxa exhibited sustained abundance
141 changes (Figure S3c).
142 Next, we analyzed gut-specific metabolic modules using GOmixer. Again, fasting induced
143 pronounced alterations that largely reverted to baseline during follow-up (Figure 2f). Only for
144 three modules, ketone body synthesis, osmoprotectant transport system, and
145 N-acetylneuraminate and N-acetylmannosamine degradation, fasting induced a long-lasting
146 increase when comparing baseline to follow-up (Figure 2f, Figure S4a, Supplementary Data
147 3).
148 Overall, prolonged fasting induces pronounced compositional shifts in the gut microbiome
149 which were largely reversed upon refeeding, resulting in minimal long-term deviations from
150 baseline at the 12-week follow-up. Notably, baseline alpha diversity metrics correlate with
151 the magnitude of alpha diversity changes both immediately after fasting and at follow-up.
152
153 *Prolonged fasting alters plasma and fecal metabolome*

154 We performed nuclear magnetic resonance (NMR) spectroscopy on plasma and fecal
155 samples to assess the impact of fasting, and its associated microbiome shifts on the fecal and
156 host metabolome. Principal coordinate analysis (PCA), centered on baseline values to
157 characterize post-fast changes and on post-fast values to characterize follow-up effects,
158 revealed plasma metabolome trajectories analogous to those observed in the gut
159 microbiome (Figure S4b). In line, we observed significant alterations between baseline,
160 fasting, and follow-up, with most changes reversed at follow-up (Figure S4c, Supplementary
161 Data 4). In plasma, only valine, glycine, tyrosine, and pyruvic acid exhibited sustained
162 increases from baseline to follow-up, indicating lasting effects of fasting on these metabolites
163 (Figure S4b, c).
164 Fecal metabolite profiling again revealed a pattern of alteration and reversion to baseline
165 (Figure S4d). Contradicting other previous reports on short-chain fatty acids (SCFA) in
166 fasting[5], we observed a decrease in butyrate during fasting, which was non-significant at
167 follow-up (Figure S4e, Supplementary Data 5). The only long-term effect observed in our data
168 was a decrease in choline from baseline to fasting (Figure S4e).
169 In conclusion, NMR-based metabolomics of plasma shows more consistent alterations as
170 compared to the fecal metabolome, which might be due to the different matrix or
171 intraindividual variations in gut microbiome composition.
172
173 *Prediction of sustained BMI response by multi-omics machine learning*
174 Since we observed strong intraindividual differences in response to prolonged fasting across
175 most data layers, we aimed to investigate whether the clinical response to fasting can be
176 predicted from baseline data. Since BMI showed the overall strongest long-term effect of the
177 analyzed clinical data (Figure 1), we focused on the long-term weight loss phenotype. Using

178 the waiting list control, we estimated the normal fluctuation of BMI within 12 weeks of study
179 participation. Normal fluctuation in BMI was defined as mean ± two standard deviations
180 (SD)[16], in our case -0.008 ± 0.32 kg/m^2. With this threshold, we identified 38% BMI long-term
181 responders and 62% BMI non-responders to prolonged fasting. In order to cross-validate our
182 model in publicly available datasets we focused on microbiome and clinical features over
183 NMR metabolomics[5,17]. A random forest classifier was trained on 87 features including the 50
184 most abundant species, candidate species and pathways from previous studies on prolonged
185 fasting, as well as relevant clinical metadata (Supplementary Data 6) using 80% of our data.
186 To account for the small sample size, we used leave-one-out cross-validation. The model was
187 evaluated on the remaining 20% of the dataset that was held out during training (Figure 3a).
188 The initial model achieved 66.7% accuracy with 100% sensitivity in identifying responders in
189 the test dataset. To optimize performance, we then selected key predictors using random-
190 forest feature importance, the Boruta algorithm, and backward feature elimination
191 (Figure 3b, S5c). This analysis indicated four key predictors: LDL, systolic blood pressure (BP),
192 *Faecalibacterium* sp. incerta sedis and *Oscillibacter* sp. 57_20. Those four features were used
193 to train the final model on 80% of the dataset. The refined model demonstrated improved
194 performance, achieving 83.3 % accuracy, an 80% positive predictive value, and a 100%
195 negative predictive value (Figure S5a).
196 Baseline BMI can confound weight loss predictions, so we tested for collinearity and
197 correlations between baseline BMI and our four selected features none of which reached
198 significance (Figure 3c). To further test if our four features are mere surrogate markers of
199 baseline BMI, we incorporated baseline BMI into the model which did not improve predictive
200 accuracy (Figure S5b). Furthermore, *Oscillibacter* sp. 57_20 remained the most important

201 feature. These results confirm that our final model captured biologically relevant signals
202 beyond simple baseline BMI effects.
203 Finally, we examined the abundance patterns of the model's key features within our cohort.
204 Responders exhibited significantly higher levels of *Oscillibacter* sp. 57_20 (Figure 3d), while
205 the identified *Faecalibacterium* sp. showed no significant difference (Figure 3f). Although
206 important for responder identification, we observed no significant differences in systolic
207 blood pressure or plasma LDL levels between responders and non-responders (Figure 3e, g).
208 Taken together, we identified four (two clinical and two microbiome) features that hold the
209 potential to predict long-term weight loss in response to prolonged fasting interventions.
210 Although our model performed robustly on the 20 % hold-out set, these results were
211 achieved in a very limited cohort size.
212
213 *Validation in available datasets of patients with co-morbidities*
214 To address this limitation, we next applied our model to our published metabolic syndrome
215 cohort in which patients underwent either a five-day fasting regimen followed by a DASH
216 diet or a DASH diet alone (Figure 4a)[5]. The study outcomes were assessed 12 weeks post-
217 intervention, mirroring our study's timeline. Given the greater BMI variability expected in
218 metabolic syndrome patients, we again quantified BMI fluctuation from the DASH only group
219 and subsequently defined long-term responders with a BMI reduction exceeding 0.8 kg/m^2.
220 Remarkably, our trained model predicted sustained weight loss in this study with an AUC of
221 0.85 (Figure 4b). Our model correctly classified 19 (82.6% [61.2 – 95.1%] accuracy) of the 23
222 patients and with a sensitivity and specificity of 85.7 % and 81.3 %, respectively (Figure 4b).
223 Furthermore, patients classified as responders showed a significantly higher BMI reduction at
224 12 weeks follow-up compared to non-responders (Figure 4c, d). Consistent with our

225 healthy-participant cohort, the model's predictive features exhibited only weak correlations
226 with baseline BMI, underscoring their independence from initial body mass (Fig. 4e). In
227 univariate analyses, none of the features differed significantly at baseline between
228 responders and non-responders (Figure 4f-i).
229 As further validation, we selected a recent nutritional intervention trial in multiple sclerosis
230 patients, the majority of whom exhibited normal metabolic profiles (obesity in one patient,
231 hypertension in two patients, high LDL in four patients) [17]. Notably, the study design differed
232 substantially. Patients completed two prolonged fasting cycles, interspersed with an interim
233 period of intermittent fasting (14 hrs/ day), and follow-up assessments were conducted nine
234 months apart (Figure 5a). As the control arm of this study included dietary counseling,
235 following the dietary recommendations of the German Society of Nutrition, we did not use it
236 to define average BMI shifts over nine months. Therefore, we could not calculate specificity
237 or sensitivity. Nevertheless, patients classified as responders by our model experienced
238 significantly greater weight loss than those classified as non-responders (Figure 5b). Again,
239 no significant correlations between model parameters and baseline BMI were detected in
240 this cohort (Figure 5c). Similar to the current cohort, levels of *Oscillibacter* sp. 50_27 were
241 significantly higher in responders (Figure 5e. The other features did not differ significantly
242 (Figure 5f-h).
243 Our findings indicate that baseline patient characteristics determine the magnitude of long-
244 term weight response to prolonged fasting interventions. Furthermore, the predictive model,
245 initially developed in healthy subjects, retained robust performance when applied to both
246 individuals with metabolic syndrome and to a regimen involving two separate prolonged-
247 fasting episodes.
248

249 *Metabolite associations with Oscillibacter sp. 57_20 and Faecalibacterium sp. incertae sedis*

250 Since both the *Oscillibacter* sp. 57_20 and the *Faecalibacterium* sp. identified in this study
251 were predictive of weight loss, we wanted to further understand the potential metabolite
252 profile associated with these bacteria. Therefore, we performed an exploratory correlation
253 analysis with the fecal metabolome across all visit data while blocking the visit information[18].
254 We found significant associations of *Faecalibacterium* sp. with butyrate, tryptophan, and
255 uridine (Figure 6a-c, Supplementary Data 7) as well as of *Oscillibacter* sp. 57_20 with glycerol
256 and methionine, and for uridine without reaching statistical significance (Figure 6d-f,
257 Supplementary Data 8). In summary, our data suggest that the bacterial species important
258 for the classification of long-term body weight responders modulate the metabolomic output
259 of the fecal microbiome.

260

261 **Discussion**

262 Our data show that prolonged fasting leads to long-term body weight and body fat reduction
263 after 12 weeks. Interindividual variability in response to dietary interventions poses a major
264 challenge in lifestyle interventions. Large-scale studies have shown that both host and
265 microbial factors shape individual metabolic responses, emphasizing the need for precision
266 strategies[19,20]. Using baseline microbiome and clinical data, we can predict individuals who
267 will respond to fasting with sustained weight loss, defined as a BMI reduction lower than the
268 mean minus two standard deviations of the waiting list control. Using available data from
269 similar interventions in patients with metabolic syndrome and patients with multiple
270 sclerosis, we could validate our data-driven classification approach. While *Faecalibacterium*
271 sp. incertae sedis and *Oscillibacter* sp. 57_20, were important for BMI response prediction,
272 most of the microbiome and metabolome features were characterized by transient shifts
273 induced by fasting, with subsequent return to pre-intervention states. Taken together, our
274 data implicate gut microbiota in long-term BMI changes post fasting and suggest conserved
275 effects of fasting regardless of health status.

276 On host level, prolonged fasting led to strong changes of multiple cardiometabolic risk factors
277 like LDL cholesterol, waist-to-hip ratio, and systolic and diastolic blood pressure. However, at
278 12 weeks follow-up these changes mainly reverted, indicating that prolonged fasting does
279 not exert a sustained effect in healthy individuals. These data differ from in patients with
280 metabolic syndrome with values above the healthy range[5]. Interestingly, while blood glucose
281 dropped during fasting, it increased upon refeeding during the day (6am to 10pm). Since
282 values at night (10pm to 6am) did not increase, our data suggest a mildly disturbed glucose
283 handling for the early days post-fasting. A similar phenotype was reported in the literature in
284 response to standardized meal intakes after prolonged fasting[21,22]. This was attributed to the

285 metabolism successfully switching to fatty acid and ketone oxidation and postprandial
286 carbohydrate oxidation was reduced leading to higher plasma glucose levels[21]. Since a strong
287 metabolic phenotype was expected, REE reduction was our predefined endpoint. REE in
288 fasting was studied previously mainly in healthy men[23-25] Our data shows an overall similar
289 but smaller effect, which might be due to the inclusion of healthy women and a broader
290 range of lean masses. Levels of REE reduction after 24h caloric deprivation was previously
291 associated with weight gain after 6 months in healthy individuals[26]. We could not confirm
292 these findings in our cohort for long-term weight changes after 3 months using the changes
293 in REE after 5 days of fasting (Figure S6). However, using a combination of clinical and
294 microbiome data, we were successful in predicting long-term weight loss.
295 We have shown in the past the microbiome and immune data can predict blood pressure
296 reduction in patients with metabolic syndrome in response to fasting[5]. In contrast, our study
297 in healthy participants revealed only modest effects on blood pressure. Given the well-
298 established impact of fasting on weight managemen[27], we applied a data-driven approach
299 that involved clustering participants based on BMI changes and employing a random forest
300 classifier. Our initial model, which incorporated 83 features, demonstrated high sensitivity
301 but limited specificity, iterative feature selection enabled us to identify *Faecalibacterium* sp.
302 incertae sedis, *Oscillibacter* sp. 57_20, plasma LDL levels, and systolic blood pressure as key
303 predictors. Notably, independent validations highlighted the robustness and generalizability
304 of our approach. In the Maifeld et al. cohort[5], which featured a similar study design in
305 patients with metabolic syndrome, we observed an 82.6% of responders were correctly
306 identified. In the Bahr et al. cohort[17], with a different study design incorporating intermittent
307 fasting in patients with multiple sclerosis, predicted responders exhibited higher weight loss.
308 These external validations not only reinforce the reliability of our predictive model but also

309 suggest that the gut microbiome changes associated with fasting responses are conserved
310 across diverse populations, from healthy individuals to those with metabolic disorders and
311 autoimmune disease, thereby broadening the potential applicability of fasting-based
312 interventions for weight management and metabolic health.

313 Given that baseline BMI is typically a key predictor of weight loss, we assessed its
314 confounding effect on fasting-induced BMI changes. *Oscillibacter* sp. 57_20 remained the
315 stronger predictor even when baseline BMI was included in the model, indicating that this
316 microbial species may exert an independent influence on weight regulation during fasting.
317 While we cannot fully exclude potential confounding or correlations between baseline BMI
318 and microbiome composition, to our knowledge, no prior study has directly linked
319 *Oscillibacter* sp. 57_20 with weight regulation. However, *Oscillibacter* sp. 57_20 was recently
320 identified as a keystone taxon in a similar prolonged fasting study in healthy individuals,
321 where it was implicated in the production of indole-3-propionate (I3P)[28], a protective
322 metabolite in cardiometabolic disease[29]. Future research is needed to explore the
323 mechanistic role of *Oscillibacter* spp. in host metabolism and its potential relevance in
324 personalized fasting interventions.

325 *Faecalibacterium* spp. are known SCFA producers[30]. In line, our data shows that the
326 abundance of our specific *Faecalibacterium* sp. associates with fecal butyrate levels. As
327 described previously for other *Faecalibacterium* spp.[31], the identified *Faecalibacterium* sp.
328 correlates with fecal tryptophan. Tryptophan can be catabolized by gut microbiota to indole
329 metabolites[32]. Unfortunately, due to the resolution of NMR metabolomics, we could not
330 detect specific indole metabolites like I3P. However, our data implicate that both bacteria
331 might interact in the production of tryptophan catabolites.

332 Both the *Faecalibacterium* sp. identified in this study and the *Oscillibacter* sp. 57_20
333 correlate with the nucleoside uridine. Uridine can adaptively regulate food intake in healthy
334 participants[33]. Furthermore, experimental evidence show that blood uridine levels reflect the
335 nutritional status of mice[34,35] with high uridine levels as indicators of catabolic states[34,36]. In
336 line, dietary supplementation of uridine enhanced hunger and increased caloric intake[33].
337 Microbial metabolism of uridine suggests a potential role of a gut-brain axis or influence on
338 satiety[37] in long-term BMI responders. Unfortunately, the literature concerning the other
339 metabolites of interest correlating with *Oscillibacter* sp. 57_20, glycerol and methionine is
340 sparse. While we controlled our analysis for abundance shifts at different visits, we could not
341 control the false discovery rate in this exploratory setting. Future confirmatory studies are
342 needed to further investigate the metabolite spectra of the identified *Faecalibacterium* sp.
343 and *Oscillibacter* sp. 57_20.
344 Overall, the gut microbiome and metabolome exhibited a consistent pattern of fasting-
345 induced alterations and nearly complete reversion to baseline at follow-up. Previous studies
346 have consistently reported an enrichment of beneficial bacteria such as *F. prausnitzii* [38-40], as
347 well as *Roseburia* and *Coprococcus* species, other known SCFA producers[41-43]. Our data only
348 partly overlaps with these reports, as we observed no alterations to *F. prausnitzii*, alongside a
349 decrease in *Roseburia* spp. and *Coprococcus* spp. However, we observed an increase in one
350 *Butyricicoccus* sp., known butyrate producers. Our functional analysis revealed an increase in
351 propionate production via kinase pathways, pointing towards an elevated SCFA production
352 potentials from coordinated activity across broader microbial community rather than single
353 species effects. The discrepancy with earlier findings may be attributed to our study's healthy
354 cohort, in which baseline levels of F. prausnitzii are likely already well-balanced. This suggests
355 that fasting might predominantly restore disturbed bacterial populations rather than altering

356 already stable communities. Suggest that fasting primarily restores imbalanced microbial
357 populations, rather than reshaping already stable communities.[44] Interestingly and consistent
358 previous studies, we did not observe overall change in alpha diversity[5,42]. However,
359 participants with lower baseline alpha diversity responded with a long-lasting increase to the
360 fasting intervention. High microbial diversity stabilizes microbiota functions during
361 perturbations[45]. In diseases usually associated with lower alpha diversity, such as obesity,
362 other fasting interventions increase alpha diversity[46]. Together, these studies reinforce the
363 hypothesis that fasting effects on alpha diversity are more pronounced in individuals with a
364 reduced microbial diversity. However, low baseline alpha diversity may also arise from
365 unaccounted external influences (e.g., lifestyle habits immediately preceding the
366 measurement).
367 Despite these promising results, our study has several limitations. First, the lack of
368 comprehensive documentation on dietary intake following the fasting intervention. Whether
369 significant weight loss was solely due to fasting or also influenced by subsequent dietary
370 modifications, a common limitation in caloric restriction studies, cannot be determined.
371 From a computational perspective, the relatively small sample size, particularly the initial test
372 dataset after splitting, poses challenges for the random forest model and feature selection[47].
373 However, the validation in two independent cohort shows the robustness of our approach[48].
374 In conclusion, our study provides compelling evidence that fasting induces substantial yet
375 reversible changes in the gut microbiome and host metabolic profiles. Importantly, a subset
376 of individuals experiences sustained weight loss. The integration of microbial and clinical
377 data not only enhanced our predictive capabilities but also unveiled novel associations, such
378 as the independent role of *Oscillibacter* sp. 57_20 and *Faecalibacterium* sp. incertae sedis in
379 weight regulation. Despite limitations related to dietary documentation and sample size,

380 these findings pave the way for future research aimed at refining personalized fasting
381 interventions. Ultimately, our work underscores the promise of leveraging gut microbiome
382 insights to tailor dietary strategies for improved metabolic health and weight management.
383

384 **Methods**

385 **Study design**

386 We performed a randomized, waitlist-controlled study (LEANER study, ClinicalTrials.gov;
387 NCT04452916) carried out at the Experimental and Clinical Research Center of Charité –
388 Universitätsmedizin in Berlin, from November 2020 to December 2022. The study protocol
389 was approved by the institutional review board of Charité – Universitätsmedizin Berlin
390 (EA1/033/20) and all participants provided written informed consent before entering the
391 study. We collected and managed study data using REDCap electronic data capture tools
392 hosted at Charité – Universitätsmedizin Berlin[49,50]. This study was exploratory, and we did not
393 calculate a pre-determined sample size. Instead, the size of the recruited cohort was
394 determined based on methodological and feasibility considerations. A general overview of
395 the study is provided in Fig. 1a.

396

397 **Eligibility criteria**

398 We included individuals aged 20-50, who were assigned male or female at birth and
399 identified as men and women, respectively; with a body mass index between 20-30 kg/m^2.
400 Exclusion criteria were heart, lung, liver, and kidney diseases requiring medical intervention,
401 prescribed medication (except oral contraceptives), postoperative phases, current or chronic
402 infection, antibiotic treatment or a fasting week within the last 6 months, habitual use of
403 dietary supplements, food intolerances, > 2 kg body weight change within the last month,
404 pregnancy, lactation, vegan diet, smoking, drug, or alcohol abuse.

405

406 **Intervention**

407 Participants received oral and written instructions on the method of prolonged fasting.
408 Expert guidance was provided by experienced nutritionists and certified fasting counselors in
409 a group setting with 5-10 participants per group. After sufficient instruction, the fasting was
410 performed individually at home, with the possibility of reaching out to the counselor at any
411 time or to connect with other group members (if patients gave consent to share this
412 information). Participants were encouraged but not required to take time off during this
413 week. Fasting was preceded by one preparation day, on which participants consumed a low-
414 calorie, fiber-rich diet, e.g. fruits, vegetables, potatoes, rice, oats.
415 During the five fasting days, participants were allowed to consume 200-250 kcal/d through
416 vegetable juices and vegetable broths. Herbal teas and water could be consumed ad libitum.
417 At the morning of fasting day 6, we performed the study visit and patients were instructed
418 for the refeeding phase. A detailed fasting plan including refeeding recommendation is
419 provided as Supplementary Table S2.
420

421 **Randomization**

422 We assigned participants randomly according to a locked list created by www.randomizer.at
423 (two treatments: waiting, fasting; 1 factor: self-reported sex; permuted blocks; block sizes 4,
424 2, 6, 4). Due to the nature of the intervention and the wait-list design, blinding was not
425 possible.
426

427 **Outcome measures**

428 We established all outcome measures in advance and did not adapt them during or after the
429 study. The primary outcome measure was resting energy expenditure (REE in kcal/d) after 5
430 days of fasting vs. baseline 1 assessed by indirect calorimetry. Secondary outcomes were

431 body composition, cardiovascular parameters, various routine blood parameters, glucose
432 variability, gut metagenome, fecal and plasma metabolome. In addition, we assessed
433 compliance and safety of fasting.
434
435 **Study center assessments**
436 The waiting group underwent assessments four times, the fasting group three times. The
437 fasting group had one baseline visit (baseline 1) and started the intervention within two to
438 eleven days afterwards, the waiting group had two baseline visits with a 12-week waiting
439 period in between (baseline 0 and baseline 1) and also started the intervention within a
440 maximum of 11 days after baseline 1. These two baselines allowed detection of random time
441 effects on the assessed outcome measures. For both groups, the next visit was on the
442 morning of the sixth fasting day directly before breaking the fast (fasting). To assess medium-
443 term effects of fasting, there was another visit after 12 weeks (follow-up). Except for the
444 additional baseline 0 in the waiting group, all assessments were identical between the
445 groups. All examinations described hereafter were performed at all study visits.
446 Assessments commenced in the morning following a 12-hour overnight fast. Participants
447 were instructed to abstain from caffeine, alcohol, and vigorous exercise for 24 hours prior to
448 the assessments.
449 Venous blood was drawn and sent to an accredited laboratory (Labor Berlin, Berlin,
450 Germany) that measured parameters of glucose and lipid metabolism, blood count,
451 electrolytes, liver enzymes, uric acid, CRP, and renal function according to international
452 standards.

453 We measured waist and hip circumference to calculate waist-to-hip ratio and determined
454 body composition (lean and fat mass) by air displacement plethysmography (Bod Pod, Life
455 Measurements, Inc., Concord, CA).
456 Indirect calorimetry was conducted following a 30 min resting period while in a supine
457 position within a thermoneutral environment for a duration of 30 min (Quark RMR, COSMED,
458 Italy). REE and respiratory exchange ratio (RER) were calculated from oxygen consumption
459 and carbon dioxide production as described elsewhere.[51]
460 Office blood pressure and heart rate were determined by five automated measurements
461 within 10 min with an upper arm cuff (Mobil-o-Graph, I.E.M. GmbH, Stolberg, Germany) in
462 the absence of study personnel.
463
464 **Fecal samples**
465 At each study visit, participants received two stool collection kits and were asked to collect
466 two samples from one stool at home as soon as possible following the study visit. One
467 sample was used for gut metagenome sequencing (OMNIgene Gut, DNA Genotek, Ottawa,
468 Canada) and the other for metabolome analysis (OMNImet Gut, DNA Genotek, Ottawa,
469 Canada). These kits allow shipment without cooling to the study center. Participants sent the
470 tubes to the study center at room temperature, where they were stored at - 80°C until
471 further processing.
472
473 **Glucose sensors**
474 We assessed glucose variability by continuous glucose monitoring over 14 days. For this,
475 participants wore a glucose sensor that measured interstitial glucose concentrations in the
476 subcutaneous tissue of the dorsal upper arm every 15 min (FreeStyle Libre Pro, Abbott,

477 Chicago, IL, USA). In contrast to the use of these sensors in diabetic patients, participants in
478 this study could not see their values during the measurement. Baseline assessment was done
479 only in the waiting group directly following baseline visit 0. Additionally, fasting assessment
480 was done in all participants during preparation, fasting and refeeding.
481
482 **Ketone and glucose measurements**
483 On the five fasting days, participants independently measured their blood concentration of
484 beta-hydroxybutyrate (BHB) and glucose twice daily using a handheld glucometer (Freestyle
485 Precision Neo, Abbott, Chicago, IL, USA), and recorded their values in a provided protocol. In
486 addition, values were stored on the device and read out later in the study center, providing
487 an objective measure of compliance.
488
489 **Fecal metagenomic sequencing**
490 *DNA isolation*
491 DNA was isolated using ZymoBIOMICS DNA Miniprep Kit (ZymoReseach Europe GmbH,
492 Freiburg, Germany). In short, an aliquot of 250 µL of stool sample from the OMNIgene Gut
493 tube was added to a ZR BasingBead Lysis Tube. The following extraction was done according
494 to the manufacturer's instructions. DNA was eluted in 100 µL RNase/DNase-free water and
495 collected in a 1.5 mL Eppendorf Tube. Total DNA concentration was measured using
496 NanoDrop ND-1000 (Peqlab Biotechnologie GmbH, Erlangen, Germany). Isolated DNA was
497 stored at - 80°C[52].
498
499 *Shotgun metagenomics*

500 Isolated DNA was shipped on dry ice to Novogene (Cambridge, UK) for shotgun metagenomic
501 DNA sequencing. In short, DNA was fragmented and subsequently underwent end repair and
502 phosphorylation. After A-tailing, adapter ligation was performed. Then 150 bp paired-ending
503 sequencing was performed on the Illumina Novaseq 6000 platform with an aimed data
504 collection of 6Gb raw data.
505
506 *Microbiome data processing*
507 Sequencing reads were mapped to the mOTUv2 (version 2.6) database, and read counts
508 were subsequently rarefied using the RTK R package (version 0.2.6.1) to standardize
509 sequencing depth across samples. Rarefaction involves randomly subsampling reads to
510 match the sample with the lowest read depth, thereby mitigating biases introduced by
511 variable sequencing depth and enabling reliable comparisons across cohorts. For the LEANER
512 (healthy) cohort, a cutoff of 3,859 reads was applied, resulting in the exclusion of one sample
513 due to insufficient sequencing depth. The same threshold was used for the Maifeld cohort[5],
514 where one sample was also excluded. In the Bahr dataset[17], applying the same rarefaction
515 criteria led to the exclusion of one sample. This consistent approach enabled reliable
516 comparisons across cohorts and increased the robustness of downstream analyses.
517
518 **Plasma metabolomics**
519 *Collection of plasma*
520 Venous blood was collected in Vacutainer® EDTA tubes (BD, Heidelberg, Germany) and
521 immediately put on crushed ice for 30 min and then centrifuged (3,000 g, 4°C, 10 min).
522 Plasma was collected and stored at - 80°C.
523

524 *Preparation of plasma for nuclear magnetic resonance spectroscopy (NMR)*

525 Plasma samples were prepared with a robotic system (SamplePro Tube, Bruker BioSpin
526 GmbH, Ettlingen, Germany) by mixing 287 µL plasma with 287 µL IVDr buffer (Bruker BioSpin
527 GmbH, Ettlingen, Germany) and adding 10 µL formic acid (240 mM) as internal standard.

528

529 *NMR measurement of plasma*

530 All NMR experiments were performed on a 600 MHz Bruker Avance III spectrometer, using a
531 triple resonance (^{1}H, ^{13}C, ^{15}N, ^{2}H lock) helium cooled cryoprobe with z-gradient. Samples
532 were handled by an automatic Bruker SampleJet sample changer (Bruker Biospin GmbH,
533 Ettlingen, Germany). Tuning and matching of the probe as well as locking and shimming of
534 the sample were performed automatically. Following the Bruker IVDr protocol for plasma
535 measurements, for each sample four different types of ^{1}H NMR spectra were acquired at 310
536 K (1D NOESY, 2D JRES, 1D CPMG, and 1D spin echo diffusion spectrum).

537

538 *Data analysis of plasma NMR spectra*

539 From the collected spectra of each specimen, 41 smaller, non-lipoprotein metabolites were
540 automatically identified and quantified using the Bruker IVDr Quantification in Plasma/Serum
541 B.I.Quant-PSTM platform. Of note, only metabolites levels not bound to proteins were
542 determined. Additionally, 112 lipoprotein parameters including various lipoprotein fractions,
543 classes and subfractions were identified and quantified using the Bruker IVDr Lipoprotein
544 Subclass Analysis B.I.LISATM platform.

545

546 **Stool metabolomics**

547 *Drying of stool samples*

548 Fecal samples from OMNImet Gut tubes were processed for metabolomics. Fecal samples (1
549 mL) were dissociated two times after adding 2.5 mL 70% isopropanol using C tubes with the
550 gentleMACS OctoDissociator (Miltenyi Biotec, Bergisch Gladbach, Germany). Aliquots of
551 dissociated samples were covered with perforated Parafilm and dried overnight in a vacuum
552 concentrator (Concentrator 5301, Eppendorf, Hamburg, Germany). Dried samples were
553 stored at - 80°C.
554
555 *Preparation of stool for NMR*
556 Dried stool samples were resuspended in 600 µL (< 10 mg dry weight), 800 µL (10-40 mg dry
557 weight) or 1,000 µL (> 40 mg dry weight) of double distilled water and 10 µL of an extraction
558 standard (Nicotinic acid at 80 mmol/L) were added. Samples were centrifuged three times
559 (12 000 x g, 4 °C, 10 min) and supernatants were transferred into a fresh vial after each
560 centrifugation in order to remove particles. Of the final supernatant, 400 µL were mixed with
561 200 µL of 0.1 mol/L phosphate buffer (pH 7.4) and 50 µL of a 0.75% (w/v) solution of 3-
562 trimethylsilyl-2,2,3,3-tetradeuteropropionate (TSP; Sigma-Aldrich, Taufkirchen, Germany),
563 which served as an internal standard, in deuterium oxide.
564
565 *NMR measurements of stool*
566 NMR experiments were conducted on the same NMR spectrometer as described for the
567 plasma analyses. Before measurement, each sample was allowed to equilibrate for 300 sec in
568 the magnet, and the probe was automatically locked, tuned, matched, and shimmed. One-
569 dimensional 1H NMR spectra were obtained at 298 K using a nuclear Overhauser
570 enhancement spectroscopy pulse sequence with solvent signal suppression by pre-saturation
571 during relaxation and mixing time. For each spectrum, 512 scans were collected into 65,536

572 data points over a 20-ppm (parts/million) spectral width using a relaxation delay of 4 sec, an
573 acquisition time of 2.66 sec, and a mixing time of 0.01 sec. Spectra were automatically
574 Fourier transformed and phase and baseline corrected.
575
576 *Data analysis of stool NMR spectra*
577 In each spectrum, a set of 41 metabolites were semi-automatically identified and relative to
578 the TSP reference signal quantified using the CHENOMX 9.02 (Chenomx Inc, Edmonton,
579 Canada) software suite. To account of potential losses during sample preparation resulting
580 data was adjusted to the extraction standard and normalized to dry weight.
581
582 **Statistical analysis**
583 Descriptive statistics for interval variables are presented as mean ± standard deviation or
584 median with interquartile range (IQR). For comparisons of delta BMI between responders
585 and non-responders, normality of variable distributions was assessed by visual check of
586 histograms and qq-plots. Mann-Whitney U-test or T-test was used as appropriate. For all
587 other data, comparisons between independent groups were performed using the Mann-
588 Whitney U test, and paired samples were compared using the Wilcoxon signed-rank test.
589 Where applicable, p-values were adjusted for multiple comparisons using either the Holm
590 method (for family-wise error control) or the Benjamini-Hochberg (BH) procedure (for false
591 discovery rate control), depending on the analytical objective.
592 Permutational Multivariate Analysis of Variance (PERMANOVA) was used to test for
593 multivariate compositional differences between groups and visits.
594 To evaluate the relationship between bacterial abundance and metabolite concentrations
595 while accounting for visit timepoint, we performed permutation-based conditional

596 independence tests. Specifically, for each metabolite, its association with Oscillibacter sp.
597 57_20 and Faecalibacterium sp. incertae sedis was tested while conditioning on the visit
598 variable, using the R package coin (version 1.4.3) with 10,000 permutations. Resulting p-
599 values were corrected for multiple testing using the Benjamini-Hochberg false discovery rate
600 (FDR) method.
601 Statistical significance was defined as $p < 0.05$ or $q < 0.1$, where applicable.

602 **Data and code availability**

603 All code, data, and scripts used in this study have been made publicly available. The code,
604 scripts and processed raw data can be accessed on Zenodo
605 (doi: https://doi.org/10.5281/zenodo.15696891). Raw sequencing data will be deposited in
606 the NCBI database upon publication.

607

608 **Acknowledgement**

609 We would like to thank Anja Mähler for designing and setting up the LEANER study, for
610 recruiting the study cohort, the entire study organization and establishing the network
611 around this fasting study. We thank Alexandra Prüß who assisted as a fasting guide in
612 carrying out study protocols. We thank Jana Czychi for her excellent technical assistance. This
613 work was funded by intramural funds of the Experimental and Clinical Research Center, a
614 cooperation between the Max Delbrück Center for Molecular Medicine in the Helmholtz
615 Association and Charité - Universitätsmedizin Berlin; and external funds from the Karl and
616 Veronica Carstens foundation (KVC 0/120/2021).
617 FP, NW, HB, DNM, WG and PJO were supported by the BMFTR (Federal Ministry of Research,
618 Technology and Space), project IDs 01EJ2202A, 01EJ2202D and 01EJ2202B (TAhRget
619 consortium). FP, NW, and SKF were supported by the European union (HORIZON-HLTH-2022-
620 STAYHLTH-02, IMMEDIATE consortium). TUPB was supported by the Berlin Center for
621 Translational Vascular Biomedicine, jointly founded by BIH, Charité - Universitätsmedizin, and
622 the Max Delbrück Center. DNM and NW were supported by the DZGIF (DZG Innovation
623 Fund), Topic "Microbiome". SKF, DNM and NW were supported by the German Research
624 Foundation (DFG), project ID 437531118 (CRC1470, projects A05, A06 and A10). SKF was

supported by the DFG project TRR412 and DZHK. AZ was was supported by the DFG, project ID 324392634 (TR221).

Author Contributions

CRediT: Conceptualization: TUPB, SB, HB, NS; Data curation: GNK, TUPB, LSB, FG, SB, HB; Formal Analysis: GNK, TUPB, UL, MM, AK, HB; Funding acquisition: TUPB, NW, PO, WG, DNM, SKF, SB, HB, NS; Investigation: KK, TS, SK, GR, VM, LB, LM, LSB, FG, FP, SB, NS; Methodology: GNK, TUPB, UL, WG, PJO, SKF, HB; Project administration: SB, HB, NS; Resources: NW, AZ, PO, WG, DNM, SKF, SB, HB, NS; Software: GNK, TUPB, UL, AK, SKF; Supervision: TUPB, UL, AZ, PO, WG, DNM, SKF, SB, HB, NS; Validation: GNK, TUPB, LSB, FG, FP, HB; Visualization: GNK, TUPB, HB; Writing – original draft: GNK, TUPB, SB, HB, NS; Writing – review & editing: GNK, TUPB, KK, TS, SK, UL, GR, VM, LB, LM, MM, AK, LSB, FG, FP, NW, AZ, PO, WG, DNM, SKF, SB, HB, NS.

Conflict of interest

NS has received speaker honoraria from Teva GmbH, Alexion Pharma Germany GmbH and Roche Pharma AG. The other authors declare no competing interests.

642 **Tables**

643 **Table 1.** Baseline characteristics of healthy participants depending on their randomization to
644 fasting and waiting control arm. Data are given as means (SD). p-values fasting vs. waiting by
645 t-test. BMI, body mass index; eGFR, estimated glomerular filtration rate; ALT, alanine
646 aminotransferase; TSH, thyroid-stimulating hormone; CRP, C-reactive protein; HbA1c,
647 glycated hemoglobin.

Variable	**All**	**Fasting**	**Waiting**	***P* value**
Number (n)	38	19	19	
Sex, female	19 / 38 (50%)	9 / 19 (47%)	10 / 19 (53%)	>0.9
Age (years)	38 (8)	39 (9)	36 (8)	0.4
BMI (kg/m^2)	25.1 (2.5)	25.0 (2.7)	25.2 (2.3)	0.7
eGFR (ml/min/1.73m^2)	102 (14)	98 (12)	106 (15)	0.1
ALT (U/l)	23.1 (8.1)	23.0 (8.2)	23.2 (8.2)	0.2
TSH (mU/l)	1.70 (0.84)	1.77 (0.91)	1.64 (0.77)	0.6
CRP (mg/dl)	0.98 (0.87)	0.78 (0.28)	1.17 (1.17)	0.2
Cholesterol (mg/dl)	182 (36)	189 (35)	175 (36)	0.2
HbA1c (mmol/mol)	33.2 (2.8)	34.2 (2.6)	32.3 (2.7)	0.03
Hemoglobin (g/dl)	14.0 (1.3)	13.8 (1.3)	14.2 (1.2)	0.41
White blood count (uL^{-1})	5.46 (1.02)	5.56 (0.96)	5.37 (1.09)	0.6
Thrombocytes (uL^{-1})	240 (42)	238 (63)	239 (54)	0.9

648

649 **Figure Legends**

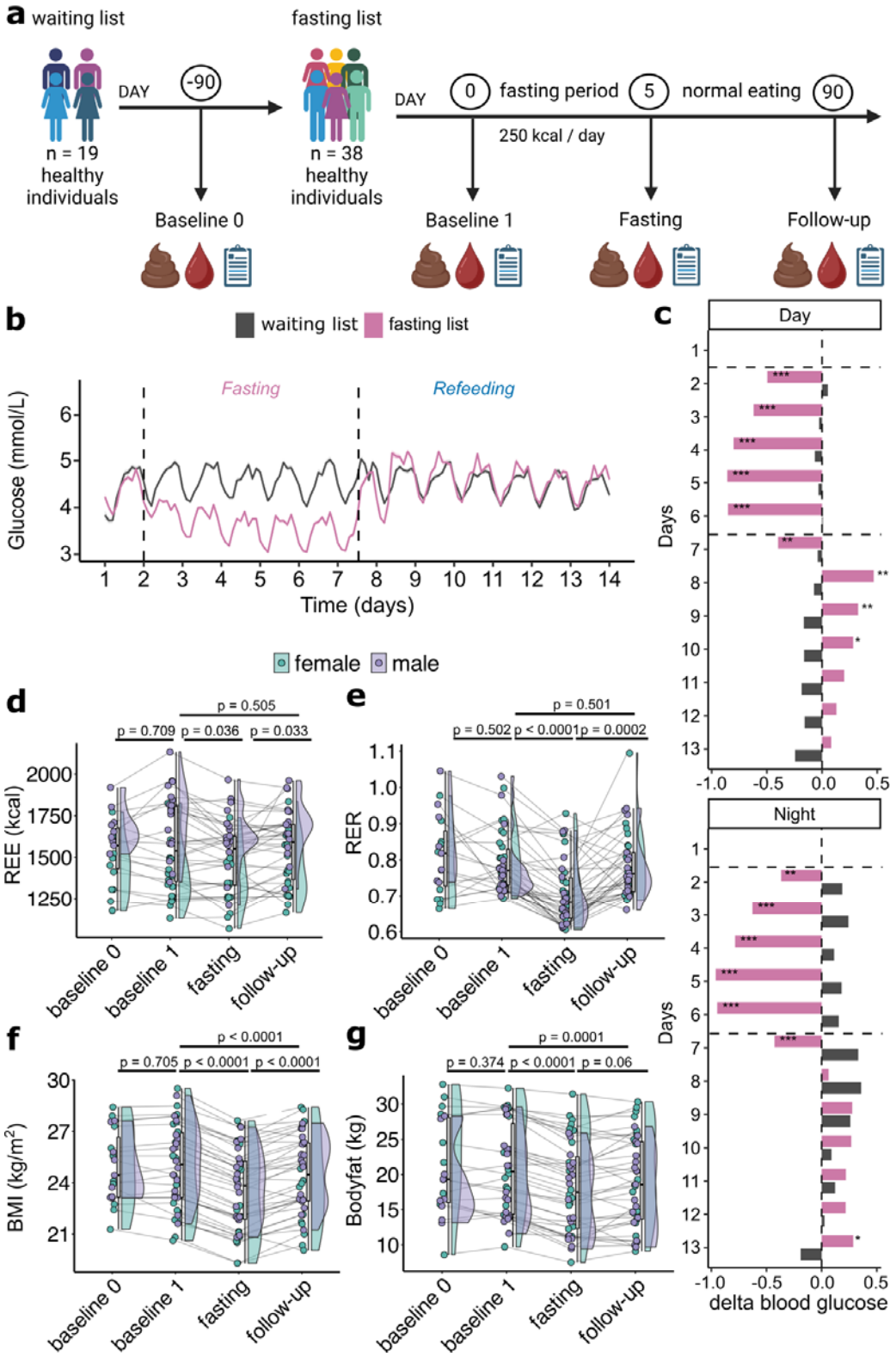

650

651 **Figure 1. Physiological effects of prolonged fasting in healthy individuals. a)** Schematic

652 overview of the randomized waitlist-controlled trial. A total of 38 healthy participants were

653 recruited. The first 19 participants immediately underwent prolonged fasting, while the
654 remaining 19 served as a waitlist control group. After the initial intervention period, the
655 waitlist group also underwent the same prolonged fasting protocol, resulting in a complete
656 dataset of 38 participants undergoing prolonged fasting. The fasting intervention consisted of
657 a 5-day period with 250 kcal/day, preceded and followed by baseline and follow-up visits at
658 days 0, 5, and 90. Stool, blood, and clinical data were collected at each visit. The waitlist
659 group was assessed at an additional baseline (day -90) to control for temporal fluctuations.
660 **b)** Glucose time series measured by continuous intradermal monitoring starting one day
661 prior to fasting (pink) or at baseline for the waiting list control (grey). **c)** Quantification of
662 absolute changes in mmol/L during the mean daytime (6am to 10pm) glucose levels (top)
663 and night (10pm to 6am) glucose levels (bottom) as changes compared to the individual
664 baseline (day 1). Paired t-test with Benjamini-Hochberg false discovery rate correction (BH-
665 FDR), *q<0.1, **q < 0.01, ***q < 0.001. **d)** Resting energy expenditure (REE), **e)** respiratory
666 exchange ratio (RER), **f)** body mass index (BMI), and **g)** body fat percentage at the different
667 study visits. Each point represents one participant, lines connect individuals, boxplot (middle)
668 for all participants, violins (right side) and dots coloured by sex. P-values are from Wilcoxon
669 signed-rank tests and were corrected using the Holm method.
670

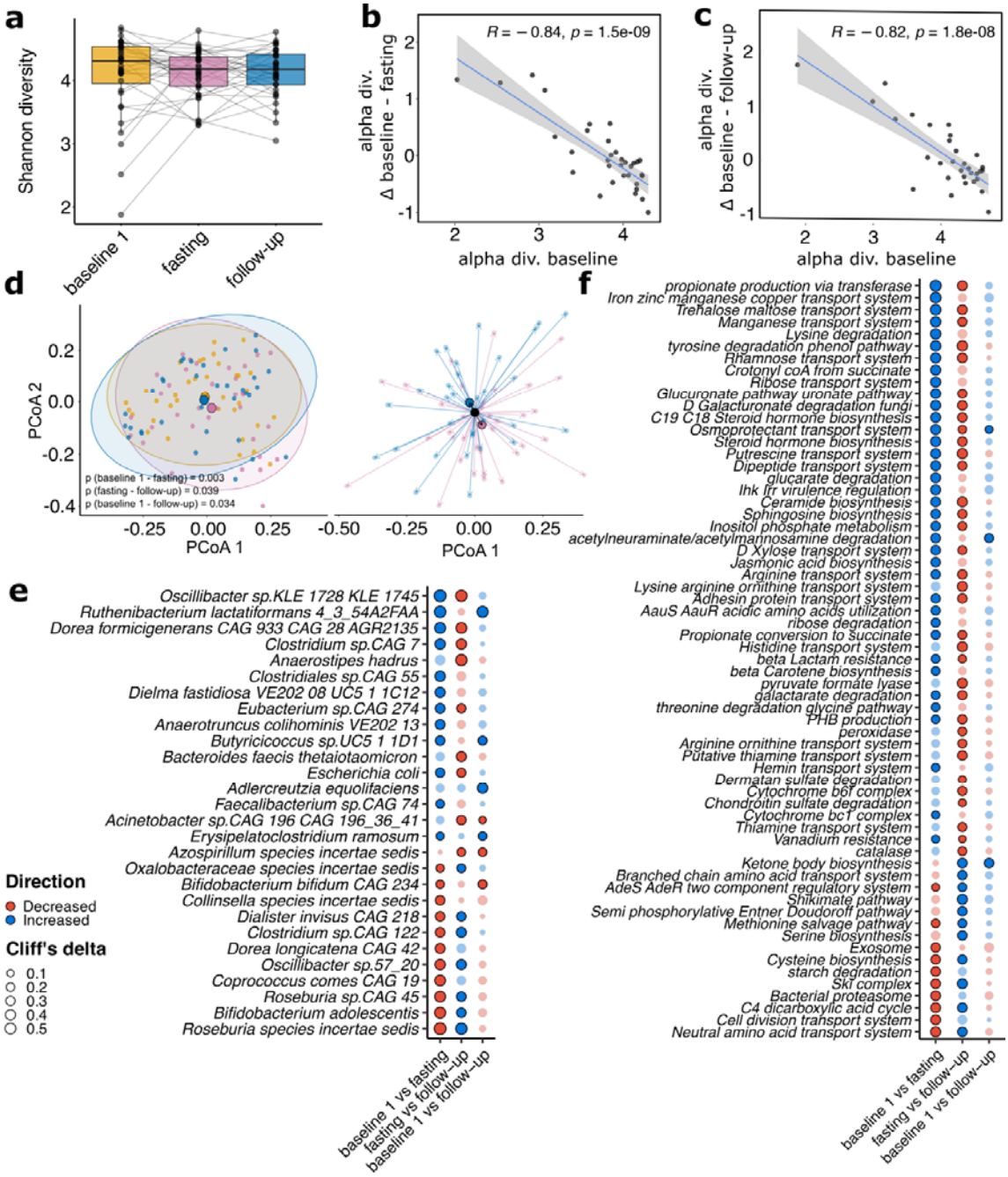

Figure 2. Prolonged fasting induces transient alterations in gut microbiome composition and function. a) Alpha diversity as measured by Shannon index for the study visits. Correlation of Shannon index at baseline with changes in Shannon index immediately **b)** post-fasting and **c)** at 12-week follow-up, indicating that baseline diversity predicts microbiome responsiveness. **d)** Principal coordinate analysis (PCoA) based on Bray–Curtis dissimilarity (naïve, left) and centered on baseline visit for fasting effect and on fasting visit

678 for post-fasting effect (right) show a transient shift in overall microbial composition after
679 fasting (pink), which partially reverts at follow-up (blue). Ellipses represent 95% confidence
680 intervals p-values from PERMANOVA. Dot plots showing differential abundant **e)** species
681 (taxonomic level) and **f)** gut metabolic modules (functional level). Dots show fasting effects,
682 follow-up effects and study effects, transparency indicates non-significant findings (q>0.1),
683 dot size shows absolute Cliff's delta, color shows directionality. Significance by Wilcoxon
684 signed-rank test with Benjamini–Hochberg false discovery rate correction.
685

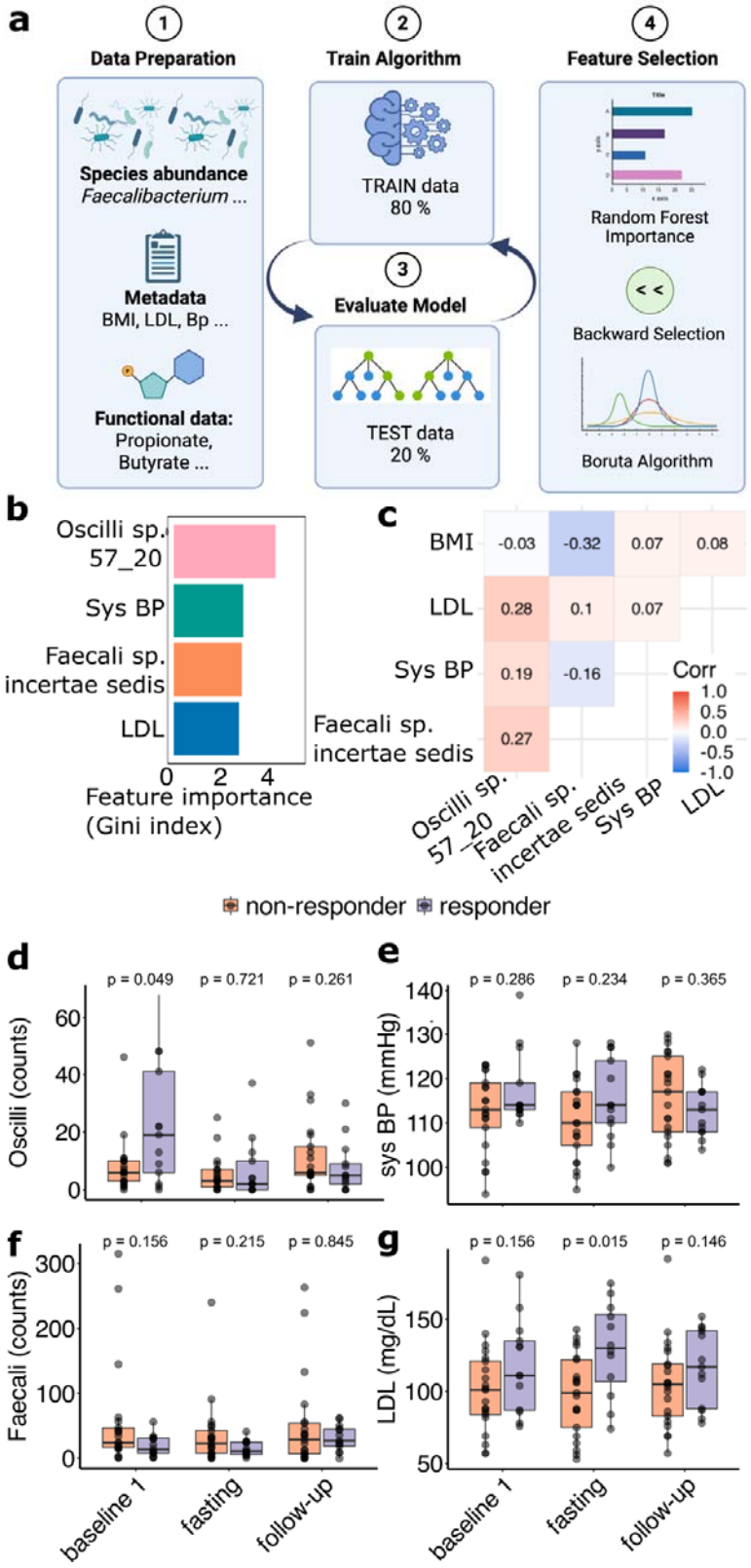

Figure 3. Machine learning model predicts sustained BMI response to prolonged fasting using clinical and microbiome features. a) Schematic overview of the multi-*omics* feature

689 selection and classification pipeline. Baseline species abundances, clinical metadata, and
690 functional modules were used to train a random forest classifier. Important features were
691 selected through recursive feature elimination, Boruta algorithm, and backward selection. **b)**
692 Final model includes four top-ranked features: *Faecalibacterium* sp. incertae sedis,
693 *Oscillibacter sp. 57_20*, LDL cholesterol, and systolic blood pressure. **c)** Correlation heatmap
694 of the selected features showing independence from baseline BMI. R-values from Spearman
695 correlation **d)** Boxplots of the four selected features at baseline, comparing BMI responders
696 and non-responders, dots show individual patients. P-values by Mann-Whitney-U-test.
697 Oscilli, *Oscillibacter sp. 57_20*; Faecali, *Faecalibacterium sp.* incertae sedis; LDL, Low-density
698 lipoprotein cholesterol; sys BP, systolic blood pressure.
699

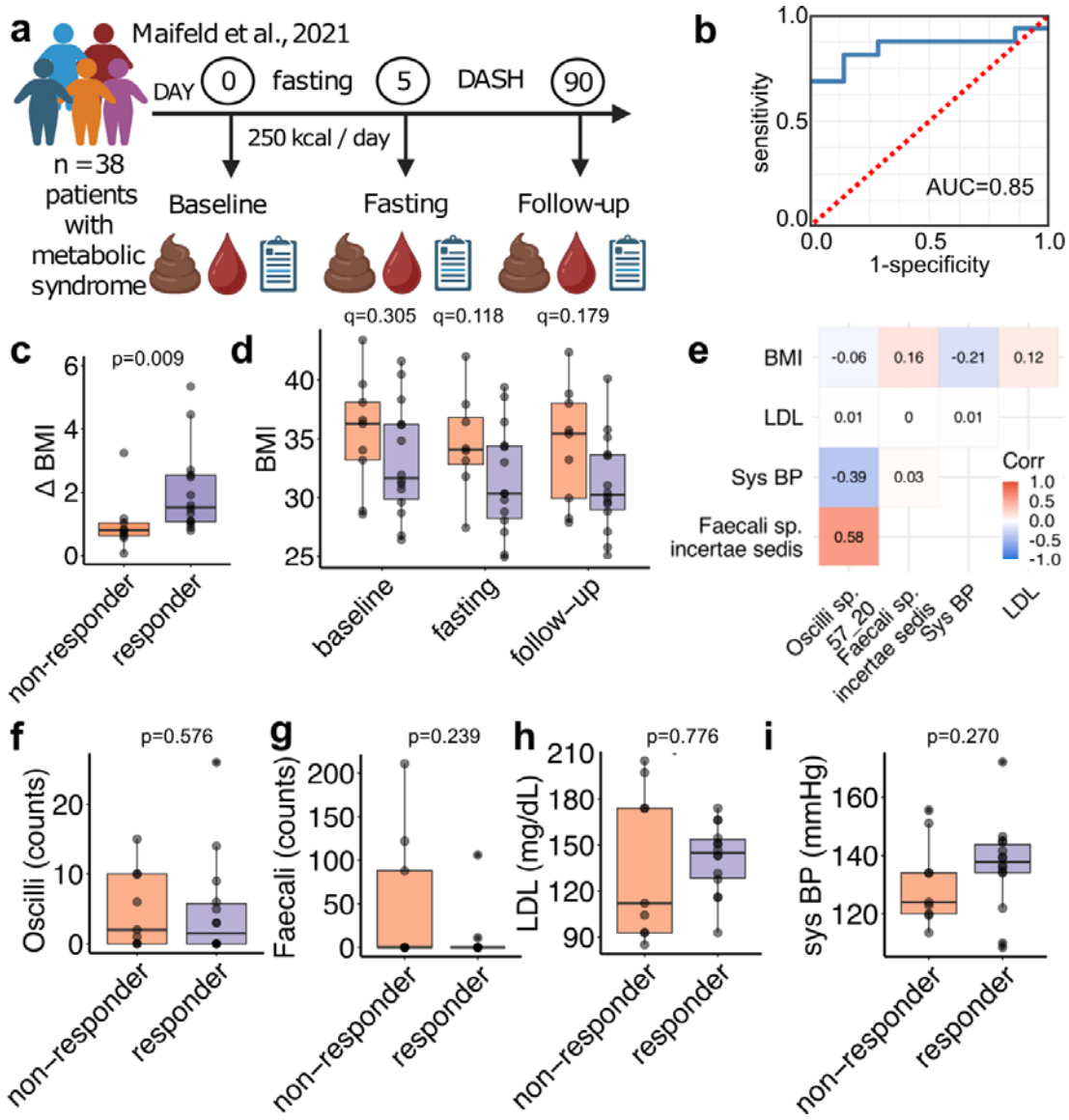

Figure 4. Validation of BMI response prediction model in a fasting cohort of patients with metabolic syndrome. a) Schematic of the Maifeld et al. (2021) study: 5-day fasting followed by a DASH diet in individuals with metabolic syndrome (n = 38), with BMI follow-up after 12 weeks. **b)** Receiver operating characteristic (ROC) curve of model performance in the Maifeld cohort, showing good predictive accuracy (AUC = 0.85). **c)** BMI reduction at follow-up of patients classified as responder or non-responder by the prediction model. p-value by one-tailed unpaired t-test. **d)** BMI over the course of the study, split by participants classified as responders or non-responders. Each point represents a participant. P-values are from paired

709 Wilcoxon signed-rank tests and were corrected for multiple comparisons using the
710 Benjamini-Hochberg false discovery rate (FDR-BH) method. **e)** Correlation heatmap of model
711 features (*Oscillibacter sp. 57_20*, *Faecalibacterium sp.* incertae sedis, LDL, systolic blood
712 pressure) within the Maifeld dataset. Features used for classification at baseline: **f)**
713 *Oscillibacter sp. 57_20*, **g)** *Faecalibacterium sp.* incertae sedis, **h)** LDL, and **i)** systolic blood
714 pressure. Oscilli, *Oscillibacter sp. 57_20*; Faecali, *Faecalibacterium sp.* incertae sedis; LDL,
715 Low-density lipoprotein cholesterol; sys BP, systolic blood pressure.
716

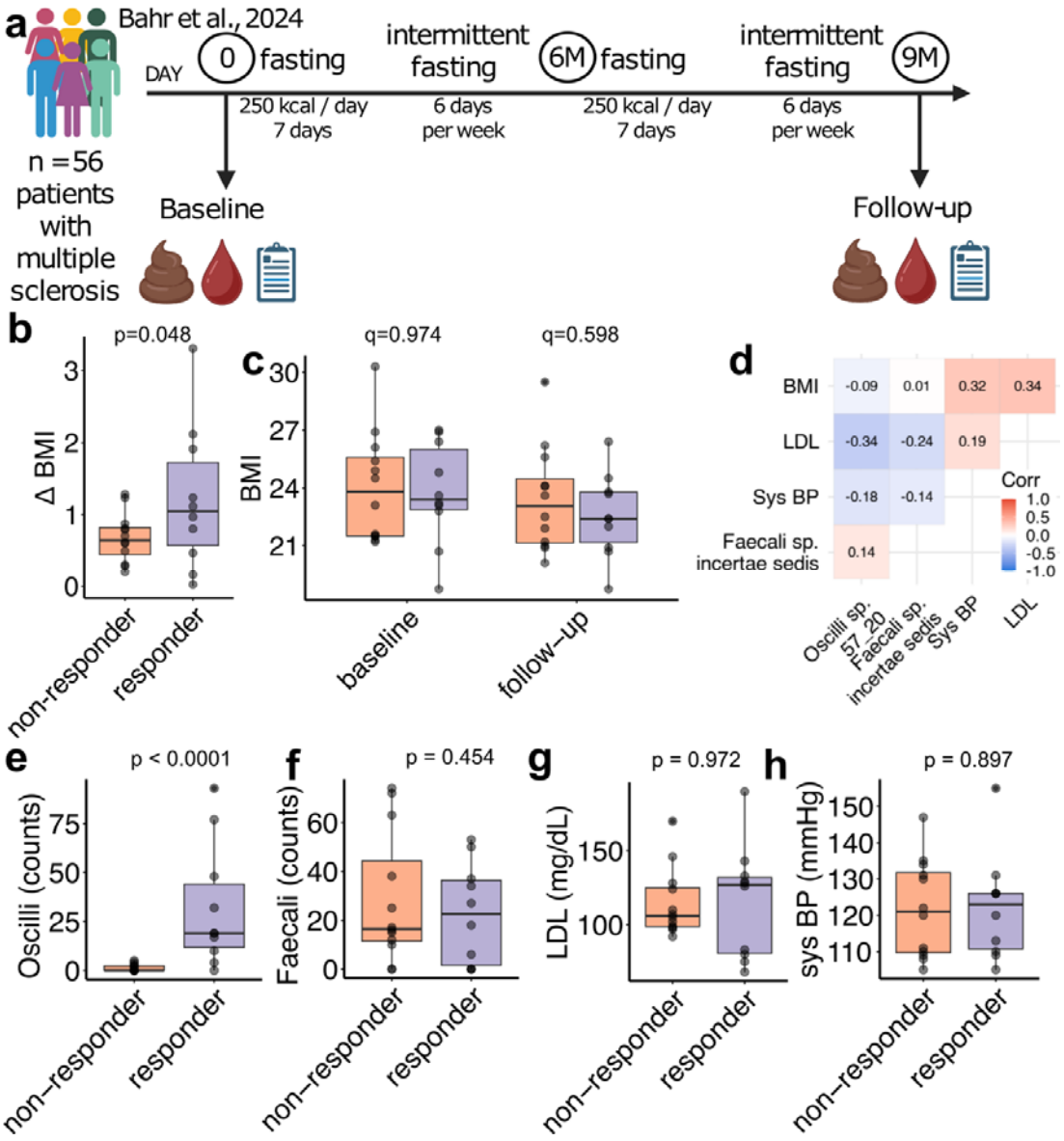

Figure 5. Validation of BMI response prediction model in a fasting cohort of patients with multiple sclerosis. a) Schematic of the Bahr et al. (2024) study: two 7-day fasting periods and intermittent fasting in individuals with multiple sclerosis (n = 56), over a 9-month period. **b)** BMI reduction at follow-up of patients classified as responder or non-responder by the prediction model. p-value by one-tailed unpaired t-test. **c)** BMI reduction at follow-up of patients classified as responder or non-responder by the prediction model. p-value by one-tailed unpaired t-test. **d)** BMI over the course of the study, split by participants classified as responders or non-responders. Each point represents a participant. P-values are from paired

726 Wilcoxon signed-rank tests and were corrected for multiple comparisons using the
727 Benjamini-Hochberg false discovery rate (FDR-BH) method. **d)** Correlation matrix of selected
728 features in the Bahr dataset. Features used for classification at baseline: **f)** *Oscillibacter sp.*
729 *57_20*, **g)** *Faecalibacterium sp.* incertae sedis, **h)** LDL, and **i)** systolic blood pressure. Oscilli,
730 *Oscillibacter sp. 57_20*; Faecali, *Faecalibacterium sp.* incertae sedis; LDL, Low-density
731 lipoprotein cholesterol; sys BP, systolic blood pressure.
732

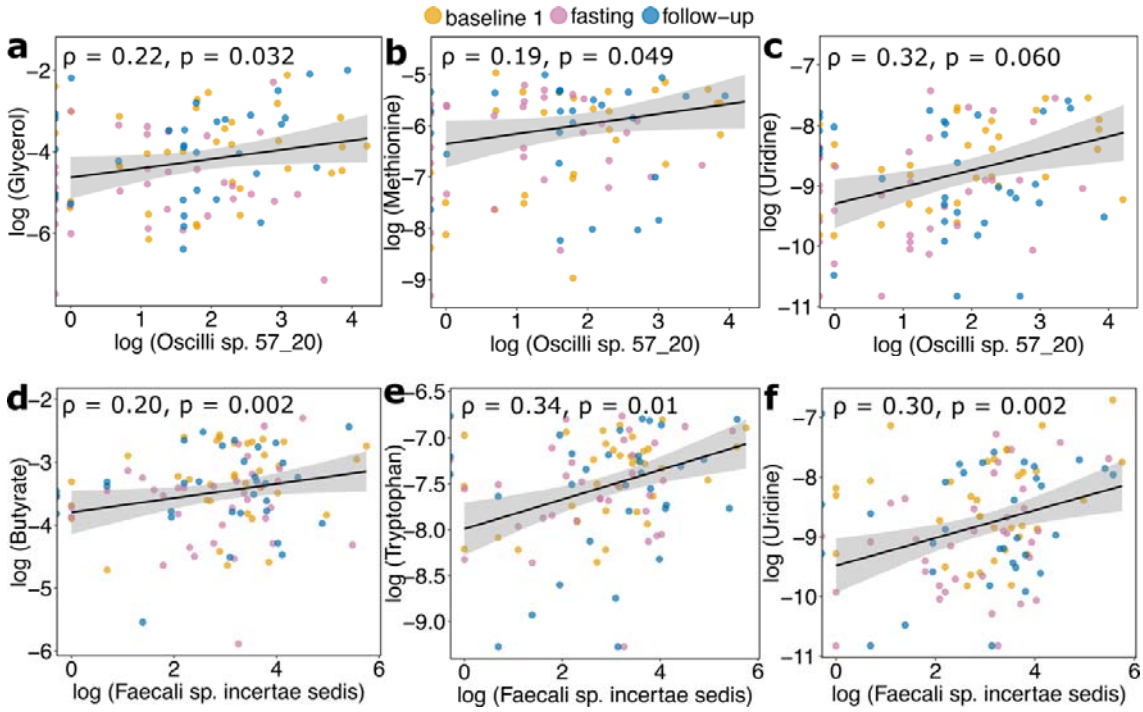

Figure 6. Oscillibacter sp. 57_20 and Faecalibacterium sp. incertae sedis abundance correlates with fecal metabolome. Correlation of Oscillibacter (Oscilli) sp. 57_20 abundance with fecal **a)** glycerol, **b)** methionine, and **c)** uridine levels. Correlation of Faecalibacterium (Faecali) sp. incertae sedis abundance with fecal **d)** butyrate, **e)** tryptophan, and **f)** uridine levels. R-values from Spearman's correlation. P-values from permutation-based independence test screening for associations of species with metabolites while blocking effects of study visits. Abbreviations: Oscilli: *Oscillibacter sp. 57_20*; Faecali: *Faecalibacterium sp.* incertae sedis.

743 **References**

744 1 Di Francesco, A., Di Germanio, C., Bernier, M. & de Cabo, R. A time to fast. *Science*
745 **362**, 770-775 (2018). https://doi.org:10.1126/science.aau2095
746 2 Brandhorst, S. *et al.* Fasting-mimicking diet causes hepatic and blood markers changes
747 indicating reduced biological age and disease risk. *Nat Commun* **15**, 1309 (2024).
748 https://doi.org:10.1038/s41467-024-45260-9
749 3 Gewecke, K. *et al.* Long-term fasting induces a remodelling of fatty acid composition
750 in erythrocyte membranes. *Eur J Clin Invest*, e14382 (2025).
751 https://doi.org:10.1111/eci.14382
752 4 Koppold, D. A. *et al.* International consensus on fasting terminology. *Cell Metab* **36**,
753 1779-1794 e1774 (2024). https://doi.org:10.1016/j.cmet.2024.06.013
754 5 Maifeld, A. *et al.* Fasting alters the gut microbiome reducing blood pressure and body
755 weight in metabolic syndrome patients. *Nat Commun* **12**, 1970 (2021).
756 https://doi.org:10.1038/s41467-021-22097-0
757 6 Cignarella, F. *et al.* Intermittent Fasting Confers Protection in CNS Autoimmunity by
758 Altering the Gut Microbiota. *Cell Metab* **27**, 1222-1235 e1226 (2018).
759 https://doi.org:10.1016/j.cmet.2018.05.006
760 7 Choi, I. Y. *et al.* A Diet Mimicking Fasting Promotes Regeneration and Reduces
761 Autoimmunity and Multiple Sclerosis Symptoms. *Cell Rep* **15**, 2136-2146 (2016).
762 https://doi.org:10.1016/j.celrep.2016.05.009
763 8 de Groot, S. *et al.* Fasting mimicking diet as an adjunct to neoadjuvant chemotherapy
764 for breast cancer in the multicentre randomized phase 2 DIRECT trial. *Nat Commun*
765 **11**, 3083 (2020). https://doi.org:10.1038/s41467-020-16138-3
766 9 Ratiner, K., Ciocan, D., Abdeen, S. K. & Elinav, E. Utilization of the microbiome in
767 personalized medicine. *Nat Rev Microbiol* **22**, 291-308 (2024).
768 https://doi.org:10.1038/s41579-023-00998-9
769 10 von Schwartzenberg, R. J. *et al.* Caloric restriction disrupts the microbiota and
770 colonization resistance. *Nature* **595**, 272-277 (2021). https://doi.org:10.1038/s41586-
771 021-03663-4
772 11 Murthy, V. L. *et al.* Metabolic liability for weight gain in early adulthood. *Cell Rep Med*
773 **5**, 101548 (2024). https://doi.org:10.1016/j.xcrm.2024.101548

774 12 Jiang, Z. *et al.* Human gut microbial aromatic amino acid and related metabolites
775 prevent obesity through intestinal immune control. *Nat Metab* **7**, 808-822 (2025).
776 https://doi.org:10.1038/s42255-025-01246-5
777 13 Hill, D. A. *et al.* Metagenomic analyses reveal antibiotic-induced temporal and spatial
778 changes in intestinal microbiota with associated alterations in immune cell
779 homeostasis. *Mucosal Immunol* **3**, 148-158 (2010).
780 https://doi.org:10.1038/mi.2009.132
781 14 Rakoff-Nahoum, S., Paglino, J., Eslami-Varzaneh, F., Edberg, S. & Medzhitov, R.
782 Recognition of commensal microflora by toll-like receptors is required for intestinal
783 homeostasis. *Cell* **118**, 229-241 (2004). https://doi.org:10.1016/j.cell.2004.07.002
784 15 Zheng, J. *et al.* Noninvasive, microbiome-based diagnosis of inflammatory bowel
785 disease. *Nat Med* **30**, 3555-3567 (2024). https://doi.org:10.1038/s41591-024-03280-4
786 16 Ozarda, Y. *et al.* Protocol and standard operating procedures for common use in a
787 worldwide multicenter study on reference values. *Clin Chem Lab Med* **51**, 1027-1040
788 (2013). https://doi.org:10.1515/cclm-2013-0249
789 17 Bahr, L. S. *et al.* Fasting, ketogenic and anti-inflammatory diets stabilized active
790 relapsing-remitting multiple sclerosis over 18 months – a randomized, controlled
791 study. *medRxiv*, 2024.2008.2013.24311863 (2024).
792 https://doi.org:10.1101/2024.08.13.24311863
793 18 Hothorn, T., Hornik, K., van de Wiel, M. A. & Zeileis, A. Implementing a Class of
794 Permutation Tests: The coin Package. *Journal of Statistical Software* **28**, 1 - 23 (2008).
795 https://doi.org:10.18637/jss.v028.i08
796 19 Berry, S. E. *et al.* Human postprandial responses to food and potential for precision
797 nutrition. *Nat Med* **26**, 964-973 (2020). https://doi.org:10.1038/s41591-020-0934-0
798 20 Zeevi, D. *et al.* Personalized Nutrition by Prediction of Glycemic Responses. *Cell* **163**,
799 1079-1094 (2015). https://doi.org:10.1016/j.cell.2015.11.001
800 21 Horton, T. J. & Hill, J. O. Prolonged fasting significantly changes nutrient oxidation and
801 glucose tolerance after a normal mixed meal. *J Appl Physiol (1985)* **90**, 155-163
802 (2001). https://doi.org:10.1152/jappl.2001.90.1.155
803 22 Solianik, R., Zidoniene, K., Eimantas, N. & Brazaitis, M. Prolonged fasting outperforms
804 short-term fasting in terms of glucose tolerance and insulin release: a randomised

805 controlled trial. *Br J Nutr* **130**, 1500-1509 (2023).
806 https://doi.org:10.1017/S0007114523000557
807 23 Laurens, C. *et al.* Is muscle and protein loss relevant in long-term fasting in healthy
808 men? A prospective trial on physiological adaptations. *J Cachexia Sarcopenia Muscle*
809 **12**, 1690-1703 (2021). https://doi.org:10.1002/jcsm.12766
810 24 Dai, Z. *et al.* Effects of 10-Day Complete Fasting on Physiological Homeostasis,
811 Nutrition and Health Markers in Male Adults. *Nutrients* **14** (2022).
812 https://doi.org:10.3390/nu14183860
813 25 Triffoni-Melo, A. T., Suen, V. M. M., Resende, C. M. M., Braga, C. B. M. & Diez-Garcia,
814 R. W. Resting energy expenditure adaptation after short-term caloric restriction in
815 morbidly obese women. *Rev Nutr* **28**, 505-511 (2015). https://doi.org:10.1590/1415-
816 52732015000500005
817 26 Schlogl, M. *et al.* Energy Expenditure Responses to Fasting and Overfeeding Identify
818 Phenotypes Associated With Weight Change. *Diabetes* **64**, 3680-3689 (2015).
819 https://doi.org:10.2337/db15-0382
820 27 Mohr, A. E. *et al.* Gut microbiome remodeling and metabolomic profile improves in
821 response to protein pacing with intermittent fasting versus continuous caloric
822 restriction. *Nat Commun* **15**, 4155 (2024). https://doi.org:10.1038/s41467-024-
823 48355-5
824 28 Ducarmon, Q. *et al.* Long-term fasting remodels gut microbial metabolism and host
825 metabolism. *bioRxiv*, 2024.2004.2019.590209 (2024).
826 https://doi.org:10.1101/2024.04.19.590209
827 29 Wang, Y. C. *et al.* Indole-3-Propionic Acid Protects Against Heart Failure With
828 Preserved Ejection Fraction. *Circ Res* **134**, 371-389 (2024).
829 https://doi.org:10.1161/CIRCRESAHA.123.322381
830 30 Barcenilla, A. *et al.* Phylogenetic relationships of butyrate-producing bacteria from
831 the human gut. *Appl Environ Microbiol* **66**, 1654-1661 (2000).
832 https://doi.org:10.1128/AEM.66.4.1654-1661.2000
833 31 Essex, M. *et al.* Gut microbiota dysbiosis is associated with altered tryptophan
834 metabolism and dysregulated inflammatory response in COVID-19. *NPJ Biofilms*
835 *Microbiomes* **10**, 66 (2024). https://doi.org:10.1038/s41522-024-00538-0

836 32 Roager, H. M. & Licht, T. R. Microbial tryptophan catabolites in health and disease.
837 *Nat Commun* **9**, 3294 (2018). https://doi.org:10.1038/s41467-018-05470-4
838 33 Hanssen, R. *et al.* Circulating uridine dynamically and adaptively regulates food intake
839 in humans. *Cell Rep Med* **4**, 100897 (2023).
840 https://doi.org:10.1016/j.xcrm.2022.100897
841 34 Deng, Y. *et al.* An adipo-biliary-uridine axis that regulates energy homeostasis. *Science*
842 **355** (2017). https://doi.org:10.1126/science.aaf5375
843 35 Steculorum, S. M. *et al.* Hypothalamic UDP Increases in Obesity and Promotes
844 Feeding via P2Y6-Dependent Activation of AgRP Neurons. *Cell* **162**, 1404-1417 (2015).
845 https://doi.org:10.1016/j.cell.2015.08.032
846 36 Deng, Y. *et al.* Adipocyte Xbp1s overexpression drives uridine production and reduces
847 obesity. *Mol Metab* **11**, 1-17 (2018). https://doi.org:10.1016/j.molmet.2018.02.013
848 37 Han, H. *et al.* From gut microbiota to host appetite: gut microbiota-derived
849 metabolites as key regulators. *Microbiome* **9**, 162 (2021).
850 https://doi.org:10.1186/s40168-021-01093-y
851 38 Ali, I. *et al.* Ramadan Fasting Leads to Shifts in Human Gut Microbiota Structured by
852 Dietary Composition. *Front Microbiol* **12**, 642999 (2021).
853 https://doi.org:10.3389/fmicb.2021.642999
854 39 Lopez-Siles, M., Duncan, S. H., Garcia-Gil, L. J. & Martinez-Medina, M.
855 Faecalibacterium prausnitzii: from microbiology to diagnostics and prognostics. *ISME*
856 *J* **11**, 841-852 (2017). https://doi.org:10.1038/ismej.2016.176
857 40 Remely, M. *et al.* Increased gut microbiota diversity and abundance of
858 Faecalibacterium prausnitzii and Akkermansia after fasting: a pilot study. *Wien Klin*
859 *Wochenschr* **127**, 394-398 (2015). https://doi.org:10.1007/s00508-015-0755-1
860 41 Guo, Y. *et al.* Intermittent Fasting Improves Cardiometabolic Risk Factors and Alters
861 Gut Microbiota in Metabolic Syndrome Patients. *J Clin Endocrinol Metab* **106**, 64-79
862 (2021). https://doi.org:10.1210/clinem/dgaa644
863 42 Mesnage, R., Grundler, F., Schwiertz, A., Le Maho, Y. & Wilhelmi de Toledo, F. Changes
864 in human gut microbiota composition are linked to the energy metabolic switch
865 during 10 d of Buchinger fasting. *J Nutr Sci* **8**, e36 (2019).
866 https://doi.org:10.1017/jns.2019.33

867 43 Ozkul, C., Yalinay, M. & Karakan, T. Structural changes in gut microbiome after
868 Ramadan fasting: a pilot study. *Benef Microbes* **11**, 227-233 (2020).
869 https://doi.org:10.3920/BM2019.0039
870 44 Sinha, A. K. *et al.* Dietary fibre directs microbial tryptophan metabolism via metabolic
871 interactions in the gut microbiota. *Nat Microbiol* **9**, 1964-1978 (2024).
872 https://doi.org:10.1038/s41564-024-01737-3
873 45 Fassarella, M. *et al.* Gut microbiome stability and resilience: elucidating the response
874 to perturbations in order to modulate gut health. *Gut* **70**, 595-605 (2021).
875 https://doi.org:10.1136/gutjnl-2020-321747
876 46 Khan, M. N. *et al.* Intermittent fasting positively modulates human gut microbial
877 diversity and ameliorates blood lipid profile. *Front Microbiol* **13**, 922727 (2022).
878 https://doi.org:10.3389/fmicb.2022.922727
879 47 Rajput, D., Wang, W. J. & Chen, C. C. Evaluation of a decided sample size in machine
880 learning applications. *BMC Bioinformatics* **24**, 48 (2023).
881 https://doi.org:10.1186/s12859-023-05156-9
882 48 Birkenbihl, C. *et al.* Differences in cohort study data affect external validation of
883 artificial intelligence models for predictive diagnostics of dementia - lessons for
884 translation into clinical practice. *EPMA J* **11**, 367-376 (2020).
885 https://doi.org:10.1007/s13167-020-00216-z
886 49 Harris, P. A. *et al.* The REDCap consortium: Building an international community of
887 software platform partners. *J Biomed Inform* **95**, 103208 (2019).
888 https://doi.org:10.1016/j.jbi.2019.103208
889 50 Harris, P. A. *et al.* Research electronic data capture (REDCap)--a metadata-driven
890 methodology and workflow process for providing translational research informatics
891 support. *J Biomed Inform* **42**, 377-381 (2009).
892 https://doi.org:10.1016/j.jbi.2008.08.010
893 51 Mahler, A. *et al.* Increased Salt Intake Decreases Diet-Induced Thermogenesis in
894 Healthy Volunteers: A Randomized Placebo-Controlled Study. *Nutrients* **14** (2022).
895 https://doi.org:10.3390/nu14020253
896 52 Bartolomaeus, T. U. P. *et al.* Quantifying technical confounders in microbiome studies.
897 *Cardiovasc Res* **117**, 863-875 (2021). https://doi.org:10.1093/cvr/cvaa128
898